

論文 / 著書情報
Article / Book Information

Title	High-mobility electronic transport in ZnO thin films
Authors	A. Tsukazaki,A. Ohtomo,M. Kawasaki
Citation	Applied Physics Letters, Vol. 88, No. 15,
Pub. date	2006, 4
URL	http://scitation.aip.org/content/aip/journal/apl
Copyright	Copyright (c) 2006 American Institute of Physics

High-mobility electronic transport in ZnO thin films

A. Tsukazaki,^{a)} A. Ohtomo, and M. Kawasaki^{b)}

Institute for Materials Research, Tohoku University, Sendai 980-8577, Japan

(Received 16 January 2006; accepted 13 March 2006; published online 11 April 2006)

A systematic study of electronic transport properties was carried out for ZnO thin films grown on high-temperature annealed buffer layers of semi-insulating $\text{Mg}_{0.15}\text{Zn}_{0.85}\text{O}$. As functions of growth temperature and oxygen pressure during laser molecular-beam epitaxy growth, there can be seen optimum growth conditions where gross concentration of intrinsic defects is thought to be reduced. For the best qualified film, Hall mobilities of $5000 \text{ cm}^2 \text{ V}^{-1} \text{ s}^{-1}$ at 100 K and $440 \text{ cm}^2 \text{ V}^{-1} \text{ s}^{-1}$ at 300 K were recorded with the residual electron densities of 4×10^{14} and $9 \times 10^{15} \text{ cm}^{-3}$, respectively. © 2006 American Institute of Physics. [DOI: 10.1063/1.2193727]

One of the recipes was proposed by us for reproducibly fabricating *p*-type ZnO, yielding in a demonstration of blue light-emitting diodes (LEDs) composed of ZnO *p-n* junction.^{1,2} Before this breakthrough, a number of papers had postulated the synthesis of *p*-type ZnO.³ What was distinct between these two was that our study was based on the establishment of a way for making ZnO as “intrinsic” as possible by reducing defect concentration. It is well known that ZnO spontaneously exhibits *n*-type semiconducting properties because interstitial Zn (Zn_i) or O vacancy (V_O) is the most stable point defects.⁴ In reality, impurities such as H, Al, and Ga, commonly found in commercial sources, also cause the electron doping. Whatever the origins of donors are, the impurity scattering suppresses the electron mobility. The highest Hall mobility (μ_H) was reported to be $230 \text{ cm}^2 \text{ V}^{-1} \text{ s}^{-1}$ at 300 K with a peak mobility $\sim 2200 \text{ cm}^2 \text{ V}^{-1} \text{ s}^{-1}$ at 50 K for highly pure bulk single crystals grown by a vapor-phase transport technique.⁵⁻⁷ The μ_H value of ZnO thin films had been limited to $160 \text{ cm}^2 \text{ V}^{-1} \text{ s}^{-1}$ with electron concentration (n) of $3 \times 10^{16} \text{ cm}^{-3}$ at 300 K partly due to crystalline defects arising from lattice mismatch and chemical dissimilarity to substrate materials.⁸⁻¹⁰ In order to overcome these issues, we have developed a high-temperature annealed ZnO buffer (HITAB) layer prepared on (0001) ScAlMgO_4 (SCAM) substrate so as to sustain layer-by-layer growth and to reduce the crystalline defects.¹¹

In this letter, we report the growth condition dependence of the electronic properties in the ZnO thin films grown on the HITAB. We find that there are narrow but distinct and systematic windows for obtaining ZnO thin films with μ_H as high as $440 \text{ cm}^2 \text{ V}^{-1} \text{ s}^{-1}$ at 300 K and $5000 \text{ cm}^2 \text{ V}^{-1} \text{ s}^{-1}$ at 100 K, even greater than those obtained for the best bulk crystals. The results are explained in terms of the formation of intrinsic defects that can be managed by tuning the growth parameters.

$\text{ZnO}/\text{Mg}_{0.15}\text{Zn}_{0.85}\text{O}$ double layers were grown on the SCAM substrates by a laser molecular-beam epitaxy (L-MBE) system equipped with a semiconductor-laser substrate-heating system.¹² First, semi-insulating and atomically flat buffer layer of $\text{Mg}_{0.15}\text{Zn}_{0.85}\text{O}$ film was formed in order to extract the intrinsic electronic properties of ZnO grown on it. By the KrF excimer laser ablation of sintered

$\text{Mg}_{0.06}\text{Zn}_{0.94}\text{O}$ target, a 100-nm-thick $\text{Mg}_{0.15}\text{Zn}_{0.85}\text{O}$ film was deposited at 923 K in 1×10^{-6} Torr of oxygen.^{13,14} The as-grown $\text{Mg}_{0.15}\text{Zn}_{0.85}\text{O}$ film exhibited coherent in-plane lattice matching with accommodating 0.06% strain. This buffer layer was then annealed at 1273 K in 1 mTorr of oxygen, yielding in atomically flat surface with completely relaxed crystalline structure. On this semi-insulating HITAB, 1- μm -thick ZnO film was grown by the ablation of aforementioned high-purity single crystal at an oxygen pressure (P_{O_2}) of 1×10^{-7} or 1×10^{-6} Torr. Laser fluence and repetition rate were set at $1 \text{ J}/\text{cm}^2$ and 5 Hz, respectively. The growth temperature (T_g) was varied by the temperature gradient method, which allows us to grow the films in a wide range of T_g on single substrate in a parallel fashion.¹⁵ Persistent oscillation of reflection high-energy electron diffraction intensity was observed during ZnO thin film growth on the HITAB in the whole range of T_g and P_{O_2} studied in the present paper.

To minimize inhomogeneity in the electronic properties induced by T_g gradient within one measured region, resistivity and Hall measurements were performed for the array of small Hall bars ($220 \times 60 \mu\text{m}^2$).¹⁵ The Ohmic contact electrodes consisting of Au(100 nm)/Ti(10 nm) were formed by electron-beam evaporation and lift-off technique. The n and μ_H were evaluated from Hall resistivity measured with applying magnetic field up to ± 1 T. All the measurements were done with using physical properties measurement system (Quantum Design), where the samples having the resistivity higher than $50 \Omega \text{ cm}$ could hardly be measured.

The n and μ_H at 300 K for all the samples are plotted against $1/T_g$ in Figs. 1(a) and 1(b), respectively. The broken lines are merely guide to the eyes. Apparently, n for 1×10^{-6} Torr samples are systematically lower than those for 1×10^{-7} samples regardless of T_g . It is noted that the trends in n for 1×10^{-7} and 1×10^{-6} Torr films show kinks intersected by two broken straight lines having different slopes. Taking Arrhenius form for logarithmic n as a function of $1/T_g$ into account, two independent surface kinetics seem to dominate the formation of nonequilibrium defects that generate the free electrons. From the trend of μ_H shown in Fig. 1(b), one can be noticed that μ_H takes the singularly maximum values at certain T_g , which coincides with the T_g giving the kinks for n . Except for these anomalies, μ_H decreases as T_g increases, exhibiting different slopes.

^{a)}Electronic mail: tsukaz@imr.tohoku.ac.jp

^{b)}Also at Combinatorial Materials Exploration and Technology, Tsukuba 305-0044, Japan.

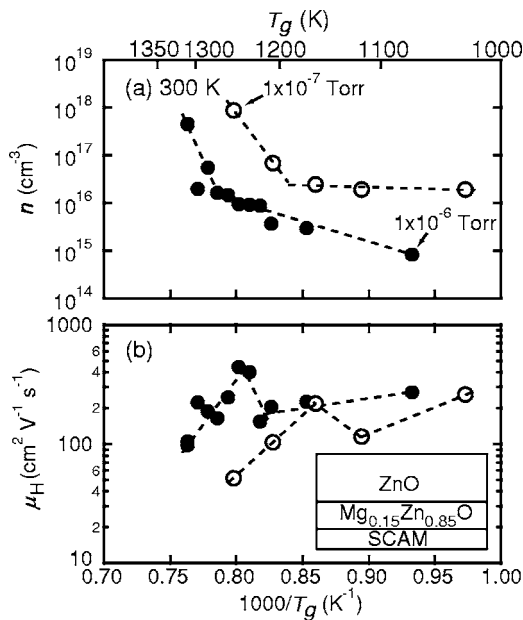


FIG. 1. (a) The growth temperature (T_g) dependence of electron concentration (n) at 300 K for ZnO thin films grown in 1×10^{-7} Torr (open circle) and 1×10^{-6} Torr (closed circle) of oxygen. (b) The T_g dependence of mobility (μ_H) at 300 K. Broken lines are merely guide to eyes.

Considering the magnitude of μ_H as a measure of the density of point defects acting as scattering centers, our results are similar to what is generally observed in MBE growth of compound semiconductors. In the case of III-V compounds, for example, there is an optimum flux ratio of III-V elements for obtaining high crystallinity with low defect concentration.¹⁶ This is also the case for MBE growth of ZnO, where high μ_H and narrow x-ray rocking curve width are simultaneously achieved for the film grown under stoichiometric condition with a Zn flux optimized for given P_{O_2} and T_g .¹⁷ This implies that for given Zn flux and P_{O_2} there should be optimum T_g , yielding in the stoichiometric condition. Although the kinetics of L-MBE growth is thought to be much more complicated,¹⁸ a number of related issues can be deduced if assuming that the T_g giving μ_H anomalies and kinks for n at fixed P_{O_2} (hereafter referred to T_{cg}) fulfill the stoichiometric conditions. We note that intrinsic donors such as Zn_i and V_O must be major defects evolving at higher T_g and lower P_{O_2} according to conventional defect chemistry. This situation seems to be realized at T_g higher than T_{cg} as steep increase of n and decrease of μ_H with increasing T_g . The fact that T_{cg} for 1×10^{-6} Torr growth is higher than that for 1×10^{-7} Torr agrees with this viewpoint. Secondly, gradual slopes of n and μ_H for T_g ranging below T_{cg} may come from the presence of acceptor-like defects in addition to the donors. Using time-resolved photoluminescence and monoenergetic positron annihilation spectroscopy, we have revealed that the concentration of Zn vacancy (V_{Zn}) increases in our films as T_g is lowered from T_{cg} .¹⁹ Similar experiment also verifies V_{Zn} assignable to an intrinsic acceptor.²⁰ Taking these facts together, the appearance of μ_H anomalies can be understood in terms of the reduction of gross concentration of intrinsic donors and acceptors.

Figure 2(a) shows the temperature dependence of n for the 1×10^{-6} Torr films as well as for a bulk single crystal.⁶ Carrier activation behavior systematically evolves with decreasing n . The activation energy was calculated from linear

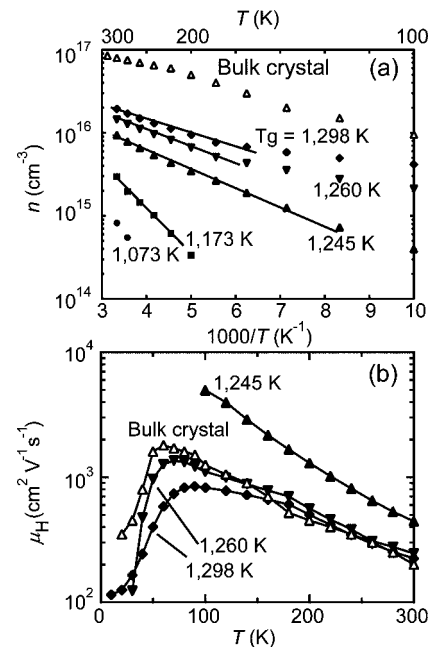


FIG. 2. (a) Temperature dependence of electron concentration (n) for ZnO thin films deposited at various growth temperatures (T_g). Data indicated by open triangles are referred from one of the best bulk single crystals (Ref. 6). The ΔE_D values are deduced from linear fit of the data; 160 meV at 1137 K, 75 meV at 1245 K, 50 meV at 1260 K, and 42 meV at 1298 K. (b) Temperature dependence of electron mobility for ZnO thin films deposited at various T_g (closed symbols). “Bulk crystal” indicated by open triangles refers to one in (a).

fitting of n near room temperature according to a formula, $n = [N_C(N_D - N_A)/2]^{1/2} \exp(-\Delta E_D/2k_B T)$, where N_C is the effective density of state at the conduction band ($\sim 4 \times 10^{18} \text{ cm}^{-3}$ at 300 K), ΔE_D is the donor activation energy, k_B is Boltzmann’s constant, and T is the absolute temperature. For the bulk single crystal, three donor levels of 30, 44, and 75 meV are assigned to $Zn_i - N_O$ or Zn_i , hydrogen, and Al_{Zn} or Ga_{Zn} , respectively.⁷ Judging from the ΔE_D evaluated from the data shown in Fig. 2(a), the electrons are mainly generated from some residual impurities in the film grown at T_{cg} , and shallow Zn_i gradually emerges with increasing T_g . The larger ΔE_D (> 100 meV) is presumably due to an anti-site such as O_{Zn} or some other deep defect or impurity state.²¹ We note that the possibility of the offset doping from the $Mg_{0.15}Zn_{0.85}O$ layers can be ruled out since the electrons are continuously frozen out as temperature decreases.

Temperature dependence of μ_H for some of the films shown in Fig. 2(a) is given in Fig. 2(b). The highest μ_H is recorded for the film grown at T_{cg} as $5000 \text{ cm}^2 \text{ V}^{-1} \text{ s}^{-1}$ at 100 K with $n = 4 \times 10^{14} \text{ cm}^{-3}$. The observation of low temperature μ_H much larger than that of the best qualified bulk single crystal leads to inclusive conclusion—the reduction of ionized impurity scattering has been accomplished in our films by the use of HITAB structure and precise tuning of growth parameters. This conclusion is also supported by systematic increase in low temperature μ_H with decreasing n (corresponding to decreasing T_g). In order to further discuss carrier scattering mechanism at low temperature and to determine upper bound of μ_H , high-resistivity films have to be characterized with using a high-impedance electrometer.

Having established the intrinsic transport properties of the ZnO thin films on HITAB, we now compare in Fig. 3 μ_H and n at 300 K of them (●) with those for the ZnO thin films

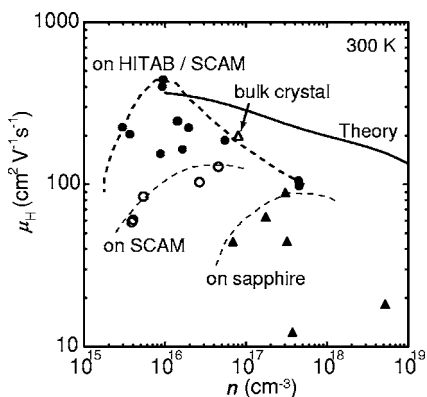


FIG. 3. The relationship of electron mobility (μ_H) between carrier concentrations (n) at 300 K in ZnO thin films grown on sapphire (closed triangles), on SCAM (open circles), and on HITAB/SCAM (closed circles). Open triangle and solid line indicate those obtained for a bulk single crystal (Ref. 6) and theoretical prediction (Ref. 22), respectively.

directly grown on (0001) sapphire (\blacktriangle) and (0001) SCAM (\circ) substrates⁸ and theoretical values (solid line) calculated by solving the Boltzmann transport equation using a variational method.²² It is clearly seen that μ_H dramatically increases and eventually reaches the theoretical limit. We note that μ_H obtained for the films grown on each substrate gives a peak value and damps rapidly as n decreases. The considerable reduction in μ_H despite of lower n seen in those grown on HITAB and SCAM is presumably due to acceptor-like defects such as V_{Zn} acting as dominant scattering center.^{19,23} Similar trend was reported for GaN, but the origin of the carrier scattering was assigned to charged dislocations.²⁴ As for our films grown on HITAB, this assignment is unlikely because full width at half maximum of x-ray rocking curve of the (0002) peak for all the films is less than the apparatus resolution (12 arc sec), giving no systematic or quantitative evidence of their presence. As a near-future challenge, the reduction of V_{Zn} and residual impurities is important for further improvement of the electrical properties. The former issue can be addressed by tuning postgrowth cooling condition.²⁰

In conclusion, we have performed systematic studies to find the optimum growth conditions for the ZnO thin films grown on HITAB, where stoichiometric conditions are thought to be fulfilled. Significant reduction in n is achieved with keeping record-breaking μ_H value, indicating that proper management of the formation of nonequilibrium defects is feasible for L-MBE growth of ZnO films. Since this process can be regarded as homoepitaxy, properly treated surface of ZnO single-crystal substrate should be able to ac-

complish the same or even better results and is more relevant to develop ZnO based LED for a practical use.

This work was supported by the MEXT Grant of Creative Scientific Research No. 14GS0204.

- ¹A. Tsukazaki, A. Ohtomo, T. Onuma, M. Ohtani, T. Makino, M. Sumiya, K. Ohtani, S. F. Chichibu, S. Fuke, Y. Segawa, H. Ohno, H. Koinuma, and M. Kawasaki, *Nat. Mater.* **4**, 42 (2005).
- ²A. Tsukazaki, M. Kumota, A. Ohtomo, T. Onuma, K. Ohtani, H. Ohno, S. F. Chichibu, and M. Kawasaki, *Jpn. J. Appl. Phys., Part 2* **21**, L643 (2005).
- ³D. C. Look, B. Clafin, Y. I. Alivov, and S. J. Park, *Phys. Status Solidi A* **201**, 2203 (2004).
- ⁴G. Neumann, *Current Topics in Materials Science* (1981), Vol. 7, Sec. 3.
- ⁵D. C. Look, D. C. Reynolds, J. R. Sizelove, R. L. Jones, C. W. Litton, G. Cantwell, and W. C. Harsch, *Solid State Commun.* **105**, 399 (1998).
- ⁶D. C. Look, J. W. Hemsky, and J. R. Sizelove, *Phys. Rev. Lett.* **82**, 2552 (1999).
- ⁷D. C. Look, G. C. Farlow, P. Reunchan, S. Limpijumngong, S. B. Zhang, and K. Nordlund, *Phys. Rev. Lett.* **95**, 225502 (2005).
- ⁸A. Ohtomo, K. Tamura, K. Saikusa, K. Takahashi, H. Koinuma, and M. Kawasaki, *Appl. Phys. Lett.* **75**, 2635 (1999).
- ⁹E. M. Kaidashev, M. Lorenz, H. von Wenckstern, A. Rahm, H. C. Semmelhack, K. H. Han, G. Benndorf, C. Bundesmann, H. Hochmuth, and M. Grundmann, *Appl. Phys. Lett.* **82**, 3901 (2003).
- ¹⁰H. Kato, M. Sano, K. Miyamoto, and T. Yao, *Jpn. J. Appl. Phys., Part 2* **42**, L1002 (2003).
- ¹¹A. Tsukazaki, A. Ohtomo, S. Yoshida, M. Kawasaki, C. H. Chia, T. Makino, Y. Segawa, T. Koida, S. F. Chichibu, and H. Koinuma, *Appl. Phys. Lett.* **83**, 2784 (2003).
- ¹²S. Ohashi, M. Lippmaa, N. Nakagawa, H. Hasegawa, H. Koinuma, and M. Kawasaki, *Rev. Sci. Instrum.* **70**, 178 (1999).
- ¹³A. Ohtomo, M. Kawasaki, T. Koida, M. Masubuchi, H. Koinuma, Y. Sakurai, Y. Yoshida, T. Yasuda, and Y. Segawa, *Appl. Phys. Lett.* **72**, 2466 (1998).
- ¹⁴A. Ohtomo, R. Shiroki, I. Ohkubo, H. Koinuma, and M. Kawasaki, *Appl. Phys. Lett.* **75**, 4088 (1999).
- ¹⁵A. Tsukazaki, H. Saito, K. Tamura, M. Ohtani, H. Koinuma, M. Sumiya, S. Fuke, T. Fukumura, and M. Kawasaki, *Appl. Phys. Lett.* **81**, 235 (2002).
- ¹⁶R. F. C. Farrow, *Molecular Beam Epitaxy* (Noyes, Park Ridge, NJ, 1995).
- ¹⁷H. Kato, M. Sano, K. Miyamoto, and T. Yao, *Jpn. J. Appl. Phys., Part 1* **42**, 2241 (2003).
- ¹⁸A. Ohtomo and H. Y. Hwang (unpublished).
- ¹⁹A. Uedono, T. Koida, A. Tsukazaki, M. Kawasaki, Z. Q. Chen, S. F. Chichibu, and H. Koinuma, *J. Appl. Phys.* **93**, 2481 (2003).
- ²⁰S. F. Chichibu, A. Uedono, A. Tsukazaki, T. Onuma, M. Zamfirescu, A. Ohtomo, A. Kavokin, G. Cantwell, C. W. Litton, T. Sota, and M. Kawasaki, *Semicond. Sci. Technol.* **20**, S67 (2005).
- ²¹D. C. Look, *Mater. Sci. Eng., B* **80**, 383 (2001).
- ²²T. Makino, Y. Segawa, A. Tsukazaki, A. Ohtomo, and M. Kawasaki, *Appl. Phys. Lett.* **87**, 022101 (2005).
- ²³F. Tuomisto, V. Ranki, K. Saarinen, and D. C. Look, *Phys. Rev. Lett.* **91**, 205502 (2003).
- ²⁴H. M. Ng, D. Doppalapudi, T. D. Moustakas, N. G. Weimann, and L. F. Eastman, *Appl. Phys. Lett.* **73**, 821 (1998).